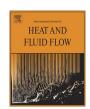
ELSEVIER

Contents lists available at SciVerse ScienceDirect

International Journal of Heat and Fluid Flow

journal homepage: www.elsevier.com/locate/ijhff



Effect of the axial scraping velocity on enhanced heat exchangers



D. Crespí-Llorens ^{a,*}, P. Martínez ^b, P. Vicente ^b, A. Viedma ^a

- ^a Dep. Ing. Térmica y de Fluidos, Universidad Politécnica de Cartagena, Dr. Fleming s/n, 30202 Cartagena, Spain
- ^b Dep. Ing. Mecánica y Energía, Universidad Miguel Hernández, Av. Universidad s/n, 03202 Elche, Spain

ARTICLE INFO

Article history:
Received 4 December 2012
Received in revised form 10 June 2013
Accepted 15 June 2013
Available online 19 July 2013

Keywords: Heat transfer enhancement Visualization study Turbulence level Numerical simulation SSHE

ABSTRACT

The flow pattern within an enhanced tubular heat exchanger equipped with a reciprocating scraping device is experimentally analysed. The insert device, specially designed to avoid fouling and to enhance heat transfer, has also been used to produce ice slurry. It consists of several circular perforated scraping discs mounted on a coaxial shaft. The whole is moved alternatively along the axial direction by a hydraulic cylinder.

The phase-averaged velocity fields of the turbulent flow have been obtained with PIV technique for both scraping semi-cycles. Special attention has been paid to the effect of the non-dimensional scraping velocity and the Reynolds number in the flow field. CFD simulations provide support for the identification of the flow patterns and the parameter assessment extension.

The results show how the scraping parameters affect the turbulence level produced in the flow and therefore the desired heat transfer enhancement.

© 2013 Elsevier Inc. All rights reserved.

1. Introduction

Insert devices have been deeply investigated (Webb, 2005) in order to improve their efficiency: heat transfer vs. pressure drop. Heat transfer enhancement techniques can be classified into *active* and *passive*. The *passive* ones, like inserted wire coils or mechanically deformed pipes, have been studied for the last 30 years and have become commercial solutions. Webb deduced from his work that *active* techniques can produce very high increases in heat transfer, especially in laminar flow.

The fouling problem of heat exchangers has a significant impact on chemical, petrochemical and food industries. Preventing fouling on heat exchanging devices is essential to avoid heat transfer inefficiencies, corrosion due to deposits formation and pressure loss, which affects the devices' performance (Bergles, 2002).

Mechanically assisted heat exchangers, where a heat transfer surface is periodically scraped by a moving element, might be used to increase heat transfer and avoid fouling. Equipment with rotating scraping blades is found in commercial practice: these devices prevent fouling and promote mixing and heat transfer. Many investigations have focused on these anti-fouling devices, studying flow pattern characteristics (Wang et al., 1999), their thermohydraulic performance (De Goede and De Jong, 1993) or scraping efficiency (Sun et al., 2004).

A particular case of fouling problem is the generation of ice slurry in heat exchangers with moving scraping devices. By cooling the outer surface of the exchanger, ice crystals are generated in its inner surface, and the moving device scraps the surface periodically to detach the ice from it. The presence of an additive in the aqueous solution reduces the freezing temperature, in order to control the proportion of ice in the solution. Ice slurries are safe, environment friendly and efficient heat transporters with a capacity of up to 150 kJ/kg. Bellas and Tassou (2005) collected their possible applications. Kauffeld et al. (2005) compared diverse ice slurry production techniques. Several researchers have studied the pressure drop and heat transfer characteristics of ice slurry flowing through compact plate heat exchangers (Bellas et al., 2002; Stamatiou et al., 2005; Norgaard et al., 2005) as well as through pipe heat exchangers (Bedecarrats et al., 2003; Lee and Lee, 2005; Lee and Sharma, 2006; Illán and Viedma, 2009b,a).

This research focuses on the analysis of the flow structures produced by the scrapers, which will significantly affect the heat transfer process. The work presents a visualization study carried-out on a heat exchanger prototype with a dynamic inserted device. The flow pattern is obtained by employing the Particle Image Velocimetry (PIV) technique and the results are shown and then compared with the flow pattern numerically obtained through a commercial CFD code. The numerical simulation will serve to find the turbulence model that best fits the experimental solution and helps to explain that particular flow pattern.

The active insert device, specially designed to enhance heat transfer and to avoid fouling, can also be used for ice slurry generation. It consists of several discs with six circumferentially

^{*} Corresponding author. Tel.: +34 605230393.

**E-mail addresses: damian.crespi@upct.es, damiancrespi@yahoo.es

(D. Crespí-Llorens).

Nomenclature D inner diameter of the acrylic pipe (m) non-dimensional radial position, $r^* = 2r/(D - d)$ d diameter of the insert device shaft (m) Re Reynolds number, $Re = \rho v_b D_h / \mu$ hydraulic diameter $D_h = D - d = 0.028$ (m) D_h non-dimensional velocity, $v^* = v/v_h$ k turbulent kinetic energy (m²/s²) L longitudinal position referenced to the centre of the Greek Symbols scraper, being positive downstream of it (mm) time elapsed between two consecutive images (s) Δt Ν number of pair of images in an experiment average displacement of the tracing particles contained Δx n number of pixels in the distance D_h in an image in an Interrogation Area between the two images of a Q flow rate (m³/s) R relation between distances in a PIV image, R = 6928.6dynamic viscosity of the fluid (Pa s) μ (pix/m) effective viscosity (Pa s) μ_{eff} radial position (m) r density of the fluid, (kg/m³) standard deviation or Root Mean Square function (RMS) S dissipation rate of turbulent kinetic energy (m²/s³) 3 T temperature (°C) fluid velocity (m/s) ν subscripts v_b bulk velocity (m/s) co-current and counter-current directions co. ct V mean velocity component (m/s) max maximum value ν' turbulent component of velocity (m/s) min minimum value \tilde{v} random error component of velocity (m/s) S scraper axial direction ν Dimensionless numbers blockage parameter, $\beta = 1 - v_s/v_h$

distributed holes on them, which are mounted on a 18 mm diameter coaxial shaft with a pitch of 5D (Fig. 1). The whole is moved alternatively along the axial direction by a hydraulic cylinder. The effects of the Reynolds number and the scraping velocity in the flow will be investigated. Furthermore, the increase of the turbulence level of the flow will be analysed and related to the potential heat transfer increase.

2. Experimental setup

The facility depicted in Fig. 2 was built in order to study the flow pattern induced by a device inserted in the exchanger tube. The main section consists of a 74 mm diameter acrylic tube installed between two reservoir tanks that stabilize the flow.

The test section is located within a distance of 15 diameters from the tube inlet in order to ensure periodic flow conditions. To improve the optical access in this section, a flat-sided acrylic box has been placed. Water is the test fluid chosen for the experiments and is also used to fill the acrylic box. The fluid is pumped through the conducts by a gear pump, regulated by a frequency converter which allows the control of its bulk velocity, measured by an electromagnetic flowmeter. The pump is composed of small gear teeth and in the experiments has always worked at frequencies over 25 Hz to ensure a stable flow. In order to control the fluid temperature, there is an electric heater in the upper reservoir tank. With the rest of the variables fixed, these two parameters determine the Reynolds number. By using water as test fluid at temperatures from 25 °C to 55 °C and flow rates of 100–1500 l/h, a Reynolds number range between 400 and 6200 can be obtained.

Particle Image Velocimetry is a broadly used technique which allows us to measure velocity patterns in a flow (Raffel et al., 2000). To that end, the flow is seeded with particles with nearly the same density of the test fluid, in this case 50 μm diameter polyamide particles have been chosen (1.016 kg/l). As shown in Fig. 3a, a laser illuminates flat slices of the flow which contain the axis of the pipe (longitudinal section). The camera is situated in orthogonal position in relation to that plane, so that it can have a front view of it. Taking two consecutive images of the particles and knowing the time gap between them, the 2-dimensional velocity field can be obtained.

The 1 mm thick plane laser light is pulsed at 100-600 Hz in order to obtain multiple pairs of images. Its wavelength is 808 nm. The $1280 \times 1024 \text{ pix}^2$ CMOS camera, together with a 16X optical zoom lens, provides images with a resolution of 0.14 mm/pix. The camera is controlled by a computer and the camera provides the synchronizing signal to the laser pulse. In the dynamic experiments, the pictures are taken in pairs, triggered by the movement of the scraping device. For each experiment, between 500 and 1000 pairs of images have been processed using the software VidPIV. Cross Correlation (C.C.) and Adaptive Cross Correlation (A.C.C.) algorithms have been used to process the acquired pictures. They have been applied to every pair of images consecutively (Scarano and Reithmuller, 2000), starting with the C.C. with an interrogation area of $32 \times 32 \text{ pix}^2$ and an overlap of 50%, followed by the A.C.C. algorithm with the same window size and finally repeating the last algorithm with a smaller window size ($16 \times 16 \text{ pix}^2$). Between the application of each algorithm and in the post-processing, a global velocity filter and an interpolation have been applied, the first one being in charge of eliminating outliers, vectors which are non-consistent with the rest in the field. Finally, results are obtained as an average of the individual results for each pair of

The laser light is 1 mm wide and 100 mm high. The PIV technique can only give good results in a region 80 mm high where the illumination quality is optimal. Velocity results are processed in three regions as shown in Fig. 1: Region A, upstream of the scraper, Region B, immediately downstream of the scraper and Region C after Region B, being an overlap of 20 mm between regions B and C. The position of each region is referenced to the scraper position as shown in Fig. 1. 500 pairs of images have been taken in the experiments in region A and 1000 pairs in the experiments in regions B and C.

All the experiments have been repeated at least 3 times to ensure high quality of the final results, which showed high repeatability once the experimental method was properly adjusted.

In dynamic experiments, the insert device has an alternative movement with constant and practically equal velocities in each direction ($|v_{s,co}-v_{s,ct}|<2\%$), with an amplitude of 200 mm (2.7 D). The shaft is moved by the hydraulic system depicted in Fig. 2. There is a distortion in the movement when changing

Download English Version:

https://daneshyari.com/en/article/655360

Download Persian Version:

https://daneshyari.com/article/655360

<u>Daneshyari.com</u>